

Isostructural Potassium and Thallium Salts of Sterically Crowded Triazenes: A Structural and Computational Study

Hyui Sul Lee,[†] Sven-Oliver Hauber,[†] Denis Vinduš,[‡] and Mark Niemeyer^{*‡}

Institut für Anorganische Chemie, Universität Stuttgart, Pfaffenwaldring 55, D-70569 Stuttgart, Germany, and Institut für Anorganische and Analytische Chemie, Johannes-Gutenberg Universität Mainz, Duesbergweg 10-14, D-55099 Mainz, Germany

Received January 8, 2008

Because of their similar cationic radii, potassium and thallium(I) compounds are usually regarded as closely related. Homologous molecular species containing either K^+ or Tl^+ are very rare, however. We have synthesized potassium and thallium salts MN_3RR' derived from the biphenyl- or terphenyl-substituted triazenes Tph_2N_3H (**1a**), $Dmp(Mph)N_3H$ (**1b**), $Dmp(Tph)N_3H$ (**1c**), and $(Me_4Ter)_2N_3H$ (**1d**) ($Dmp = 2,6-Mes_2C_6H_3$ with $Mes = 2,4,6-Me_3C_6H_2$; $Me_4Ter = 2,6-(3,5-Me_2C_6H_3)_2C_6H_3$; $Mph = 2-MesC_6H_4$; $Tph = 2-TripC_6H_4$ with $Trip = 2,4,6-Pr_3C_6H_2$). The potassium complexes **2a–d** were obtained in almost quantitative yield from the reaction of **1a–d** with potassium metal in *n*-heptane. Metalation of **1a–d** with $TiOEt$ afforded the thallium triazenides **3a–d** in high yields. All new compounds have been characterized by 1H and ^{13}C NMR spectroscopy, elemental analysis, and X-ray crystallography and for selected species by melting point (not **3b**), IR spectroscopy (**2a**, **2d**, **3a**, **3c**, **3d**), and mass spectrometry (**2a**, **3c**). In the solid-state structures of monomeric **2a** and **3a**, quasi-monomeric **2b**, **3b**, **2c**, and **3c**, and dimeric **2d** and **3d** additional metal- η^n - π -arene-interactions to the flanking arms of the biphenyl- and terphenyl groups in the triazenide ligands of decreasing hapticity n are observed. Remarkably, all homologous potassium and thallium complexes crystallize in isomorphous cells. For **2a** and **3a**, the nature of the $M-N$ and $M \cdots C(\text{arene})$ bonding was studied by density functional theory calculations.

Introduction

Thallium, the heaviest element in group 13, shows similarities to other elements in the periodic table, in particular, the alkali metals, Ag, Hg, and Pb,¹ an observation that led Dumas to describe it as the “duckbill platypus among elements”.^{2,3} For example, compounds of monovalent thallium can be compared to those of potassium (e.g., hydroxides, carbonates, sulfates) or silver (e.g., oxides, sulfides, halides).⁴ Furthermore, the similar ionic radii of Tl^+ and K^+ (1.64 Å vs 1.55 Å for 6-fold coordination)^{5,6} together with the higher affinity to enzymatic sites of the former are responsible for the easy

incorporation and the high toxicity of soluble thallium species. For this reason, there has been much interest in the use of Tl^+ as a probe in biochemical systems since thallium detection is much easier by diffraction methods⁷ or NMR spectroscopy.⁸

Although some simple thallium or potassium salts crystallize isotypically⁹ this is not the case for molecular organo-

* To whom correspondence should be addressed. E-mail: mn@lanth.de.

[†] Universität Stuttgart.

[‡] Johannes-Gutenberg Universität Mainz.

(1) Lee, A. G. *The Chemistry of Thallium*; Elsevier: Amsterdam, The Netherlands, 1971.

(2) Housecroft, C. E.; Sharpe, A. G. *Inorganic Chemistry*, 2nd ed.; Pearson: Harlow, 2005.

(3) Dumas, J. B. A. *Compt. Rend.* **1862**, 55, 866.

(4) Wiberg, N. *Holleman-Wiberg-Lehrbuch der Anorganischen Chemie*, 102nd ed.; deGruyter: Berlin, 2007.

(5) Shannon, R. D. *Acta Crystallogr.* **1976**, A32, 751.

(6) The Shannon ionic radius of Rb^+ (1.66 Å) is even closer to that of Tl^+ . However, these radii were determined with strongly polarizing anions such as O^{2-} or F^- as counterions. Therefore, as was noted before by Mudring and Rieger (ref 13), a comparison of the lattice constants of compounds with a less coordinating counteranion might be more suitable to illustrate the difference in the ionic radii, e.g., M_2PtCl_6 [$a(K_2PtCl_6) = 9.745$ Å, $a(Rb_2PtCl_6) = 9.904$ Å, and $a(Tl_2PtCl_6) = 9.775$ Å].

(7) Basu, S.; Rambo, R. P.; Strauss-Soukup, J.; Cate, J. H.; Ferré-D'Amaré, A. R.; Strobel, S. A.; Doudna, J. A. *Nat. Struct. Biol.* **1998**, 5, 986.

(8) Gill, M. L.; Strobel, S. A.; Loria, J. P. *J. Am. Chem. Soc.* **2005**, 127, 16723.

(9) For example, M_2SO_4 . The halides MX ($X = Cl, Br, I$) crystallize in the rock salt (most stable for $M = K$) and cesium chloride (most stable for $M = Tl$) structure. In addition, TlF and yellow TlI adopt distorted forms of the sodium chloride structure. See Wells, A. F. *Structural Inorganic Chemistry*, 5th ed.; Clarendon Press: Oxford, 1984.

Table 1. Selected Structural Data for Homologous K and Tl Compounds^a

compound	space group	description	intramolecular distances and angles	intermolecular distances and angles	ref
KCp	<i>P</i> 421 <i>c</i>	polymeric structure of interconnected chains	K–C 2.96–3.14 {3.05} cent–K–cent 138.0	K···C 3.33/3.39 K···K > 4.45	18
TlCp	<i>C</i> 2/ <i>c</i>	polymeric chain structure	Tl–C 2.90–3.09 {2.99} cent–Tl–cent 130.1	Tl···C > 3.89 Tl···Tl > 3.94	19
KN(SiMe ₃) ₂	<i>P</i> 2 ₁ / <i>a</i>	associated dimers	K–N 2.77/2.80 K···C 3.34/3.47 K···K 3.79	K···C 3.30/3.49 K···K > 5.51	20
TlN(SiMe ₃) ₂	<i>P</i> 2 ₁ / <i>n</i>	dimers	Tl–N 2.58 Tl···C > 3.50 Tl···Tl 3.65	Tl···C > 4.03 Tl···Tl > 3.94	21
KOMe	<i>P</i> 4/ <i>nmm</i>	double-layered structure	K–O 2.66/2.80 K···K 3.68 Tl···Tl 3.84		22
TlOMe	<i>P</i> ca2 ₁	tetrameric			23
K(18-cr-6)ClO ₄	<i>P</i> 2 ₁ / <i>c</i> ^b	K in O ₆ -plane	K–O 2.78–2.88 {2.82} K–OCIO ₃ 2.75	K–OCIO ₃ 2.85	24
Tl(18-cr-6)ClO ₄	<i>P</i> 2 ₁ / <i>c</i> ^b	Tl out of O ₆ -plane	Tl–O 2.81–3.04 {2.93} Tl–OCIO ₃ 2.94/3.04	Tl–OCIO ₃ 3.05	13

^a Average values in braces. ^b Different cell parameters are observed.

metallic or coordination compounds. As stated recently by Wiesbrock and Schmidbaur,¹⁰ thallium(I) cations often show exceedingly low coordination numbers leaving a large part of the coordination sphere seemingly unoccupied.¹¹ Using an extremely bulky terphenyl ligand it was even possible to stabilize a thallium(I) aryl with a quasi-one-coordinate metal atom.¹² By contrast, potassium cations always have their coordination sphere covered as completely and as symmetrically as possible, optimizing the Coulomb energy and interligand interactions. These differences are usually attributed to the relativistically contracted valence shell and the stereochemically active 6s² lone pair of electrons in the former.¹³ A query in the Cambridge structural database (Vers. Jan. 2007) resulted in a very limited number of structurally characterized K(I) or Tl(I) species with the same composition (Table 1). This fact most probably originates from the higher tendency of K⁺ to coordinate additional solvent molecules. For instance, the thallium cyclopentadienyls [TlC₅HMe₄],^{14a} [TlC₅Me₅],^{14b} and [TlC₅(CH₂Ph)₅],^{14c,d} the thallium pyrazolate [Tl(Ph₂pz)] (Ph₂pz = 3,5-diphenylpyrazolate),^{14e} and the thallium carboxylate [TlO₂C(2-NH₂)C₆H₄]¹⁰ are σ -donor solvent-free, whereas the corresponding potassium derivatives are commonly obtained as solvates, for example, [KC₅HMe₄(dme)],^{15a} [KC₅Me₅(thf)_{*n*}] (*n* = 1, 2),^{15b}

[KC₅(CH₂Ph)₅(thf)₃],^{15c} [K(Ph₂pz)(thf)],^{15d} or [KO₂C(2-NH₂)C₆H₄(H₂O)].^{15e} The low tendency of Tl⁺ to coordinate σ -donor solvents is nicely reflected by the crystallization behavior of the pyrazolate [Tl(Ph₂pz)].^{14e} Crystallization from benzene affords trinuclear aggregates [Tl(Ph₂pz)]₃ linked by intermolecular Tl– π – η ⁶-arene contacts whereas crystallization from 1,2-dimethoxyethane gives tetranuclear molecules [Tl(Ph₂pz)]₄ with one additional dme solvent molecule located in cavities of the structure.

In the absence of coordinating solvents, the mainly ionic potassium compounds usually aggregate via bridging donor atoms, intermolecular metal···arene interactions, or agostic metal···C–H contacts to optimize the Coulomb energy.¹⁶ Similar factors contribute to the aggregation of thallium compounds¹² which are considered less ionic, however. In addition, the aggregation behavior is influenced by the presence of weak, attractive, thalophilic⁹ interactions between the Tl(I) centers.¹⁷

Structural differences between known homologous potassium and thallium compounds (Table 1) are summarized as follows. To begin with, the solid-state structure of the [MCp] compounds (M = K,¹⁸ Tl¹⁹) can be described as a multidecker structure with two Cp rings η ⁵-coordinated to each

(10) Wiesbrock, F.; Schmidbaur, H. *J. Am. Chem. Soc.* **2003**, *125*, 3622.

(11) (a) Janiak, C. *Coord. Chem. Rev.* **1997**, *163*, 107. (b) Schulz, S. *Comprehensive Organometallic Chemistry III*; Elsevier: Oxford, 2007; Vol. 3, Chapter 7.

(12) Niemeyer, M.; Power, P. P. *Angew. Chem., Int. Ed.* **1998**, *37*, 1277.

(13) Mudring, A.-V.; Rieger, F. *Inorg. Chem.* **2005**, *44*, 6240.

(14) (a) Schumann, H.; Kucht, H.; Kucht, A.; Gorlitz, F. H.; Dietrich, A. *Z. Naturforsch.* **1992**, *B47*, 1241. (b) Werner, H.; Otto, H.; Kraus, H. *J. Organomet. Chem.* **1986**, *315*, C57. (c) Schumann, H.; Janiak, C.; Pickardt, J.; Börner, U. *Angew. Chem., Int. Ed. Engl.* **1987**, *26*, 789. (d) Schumann, H.; Janiak, C.; Khan, M. A.; Zuckerman, J. J. *J. Organomet. Chem.* **1988**, *354*, 7. (e) Deacon, G. B.; Delbridge, E. E.; Forsyth, C. M.; Skelton, B. W.; White, A. H. *J. Chem. Soc., Dalton Trans.* **2000**, 745.

(15) (a) Evans, W. J.; Giarikos, D. G.; Ziller, J. W. *J. Organomet. Chem.* **2003**, *688*, 200. (b) Evans, W. J.; Brady, J. C.; Fujimoto, C. H.; Giarikos, D. G.; Ziller, J. W. *J. Organomet. Chem.* **2002**, *649*, 252. (c) Lorberth, J.; Shin, S.-H.; Wocadlo, S.; Massa, W. *Angew. Chem., Int. Ed. Engl.* **1989**, *28*, 735. (d) Yelamos, C.; Heeg, M. J.; Winter, C. H. *Inorg. Chem.* **1998**, *37*, 3892. (e) Wiesbrock, F.; Schmidbaur, H. *J. Chem. Soc., Dalton Trans.* **2002**, 4703.

(16) (a) Smith, J. D. *Adv. Organomet. Chem.* **1999**, *43*, 354. (b) Ruhlandt-Senge, K.; Henderson, K. W.; Andrews, P. C. *Comprehensive Organometallic Chemistry III*; Elsevier: Oxford, 2007; Vol. 2, Chapter 1.

(17) (a) For selected recent examples of Tl(I) compounds with thalophilic interactions and further cited literature, see Uhl, W.; Keimling, S. U.; Klinkhammer, K. W.; Schwarz, W. *Angew. Chem., Int. Ed. Engl.* **1997**, *36*, 64. (Tl alkyl). (b) Hellmann, K. W.; Gade, L. H.; Steiner, A.; Stalke, D.; Moller, F. *Angew. Chem., Int. Ed. Engl.* **1997**, *36*, 160. (Tl amide). (c) Rheingold, A. L.; Liable-Sands, L. M.; Trofimenko, S. *Chem. Commun.* **1997**, 1691. (Tl pyrazolylborate). (d) Robert, J.; Wright, R. J.; Phillips, A. D.; Hino, S.; Power, P. P. *J. Am. Chem. Soc.* **2005**, *127*, 4794. (Tl aryls). (e) Childress, M. V.; Millar, D.; Alam, T. M.; Kreisel, K. A.; Yap, G. P. A.; Zakharov, L. N.; Golen, J. A.; Rheingold, A. L.; Doerrer, L. H. *Inorg. Chem.* **2006**, *45*, 3864. (Tl aroxides). (f) Hill, M. S.; Pongtavornpinyo, R.; Hitchcock, P. B. *Chem. Commun.* **2006**, 3720. (Tl β -diketiminato).

(18) Dinnebier, R. E.; Behrens, U.; Olbrich, F. *Organometallics* **1997**, *16*, 3855.

(19) (a) Olbrich, F.; Behrens, U. *Z. Kristallogr.—New Cryst. Struct.* **1997**, *212*, 47. (b) Dashti-Mommertz, A.; Neumüller, B.; Melle, S.; Haase, D.; Uhl, W. *Z. Anorg. Allg. Chem.* **1999**, *625*, 1828.

metal atom. The metal atoms form a zigzag chain (centroid...M...centroid = 138° [K], 130° [Tl]) and interact with two neighboring multidecker chains either via $K \cdots \eta^2-C$ or via $Tl \cdots Tl$ contacts (see the Supporting Information, Figure S1a,b). Furthermore, the silyl amides $[MN(SiMe_3)_2]$ crystallize as N-bridged dimers. In the potassium compound,²⁰ the dimers are further linked by intermolecular agostic-type $K \cdots CH_3$ contacts to a layered structure (Supporting Information, Figure S1c). However, the thallium complex²¹ shows a columnar structure in which the dimeric subunits are weakly aggregated by $Tl \cdots Tl$ contacts (Supporting Information, Figure S1d). Moreover, the salt-like $KOCH_3$ forms a double-layer structure with $KOCH_3$ units arranged perpendicular to the plane, having their methyl groups alternately on either side of the layer.²² In contrast, the molecular Tl analogue²³ crystallizes in a tetrameric heterocubane structure. Finally, crown ether complexes of the composition $[M@18-crown-6][ClO_4]$ belong to another class of compounds that do not crystallize isotypically. In the K(I) complex²⁴ the cation is located almost in the plane defined by the oxygen atoms of the crown ether whereas in the Tl(I) complex¹³ the cation resides 75 pm above this plane. According to quantum-chemical calculations an antibonding interaction of the Tl 6s electron pair with the oxygen atoms of the crown ether is responsible for this difference.¹³

In this paper, we describe the synthesis and characterization of a series of potassium and thallium salts derived from biphenyl- or terphenyl-substituted triazenes.^{25–28} Those complexes appear to be the first examples of isostructural molecular species reported for these elements.

Experimental Part

General Procedures. All manipulations were performed by using standard Schlenk techniques under an inert atmosphere of purified argon and solvents freshly distilled from Na wire or $LiAlH_4$. The triazenes Tph_2N_3H , $Dmp(Mph)N_3H$, and $Dmp(Tph)N_3H$ were synthesized as previously described.^{25,26} 3,5,3'',5''-Tetramethyl-

1,1':3',1''-terphenyl-2'-azide (Me_4TerN_3) was obtained as a pale yellow solid from Me_4TerI ,^{29a–c} *n*-butyllithium and tosyl azide^{29d} in a similar way to that used in the preparation of $DmpN_3$.^{29e} NMR spectra were recorded on Bruker AM200, AC250 or AM400 instruments and referenced to solvent resonances. IR spectra (Nujol mull, CsBr plates) have been obtained in the range 4000–200 cm^{-1} with a Perkin-Elmer paragon 1000 PC spectrometer. Mass spectra were recorded with a Varian MAT711 or Finnegan MAT95 instrument. Melting points were determined under Ar atmosphere in sealed glass tubes.

(Me_4Ter) $_2N_3H$ (1d). *n*-Butyllithium (25 mmol, 2.5 M hexane solution) was added at 0 °C to a solution of Me_4TerI (10.0 g, 24.3 mmol) in 150 mL of diethylether and stirring was continued for 2 h. The obtained clear solution of the lithium aryl was then treated with small portions of a solution of Me_4TerN_3 (7.95 g, 24.3 mmol) in 60 mL of diethylether. After warming to ambient temperature and stirring for an additional 12 h, the red-brown solution was quenched with water (200 mL). The aqueous phase was separated and extracted with diethyl ether (3 × 80 mL). The organic phases were combined, repeatedly washed with water, and dried over Na_2SO_4 . Filtration followed by solvent removal in vacuum afforded **1d** as a yellow solid. Analytically pure, pale yellow crystals were obtained by recrystallization from acetone. Yield: 10.7 g (17.4 mmol, 72%); mp: 159–160 °C (dec.). ¹H NMR (250.1 MHz, C_6D_6): δ 2.09 (s, 24H, CH_3), 6.67 (s, 4H, *p*- $C_6H_3Me_2$), 6.90 (s, 8H, *o*- $C_6H_3Me_2$), 6.99 (t, $^3J_{HH} = 7.6$ Hz, 2H, *p*- C_6H_3), 7.23 (d, $^3J_{HH} = 7.6$ Hz, 4H, *o*- C_6H_3), 8.80 (s, 1H, NH). Anal. Calcd for $C_{44}H_{43}N_3$: C, 86.09; H, 7.06; N, 6.85. Found: C, 85.64; H, 7.42; N 6.64.

KN_3Tph_2 (2a). A mixture of an excess of potassium metal and **1a** (0.903 g, 1.50 mmol) in *n*-heptane (60 mL) was stirred for 2 h, and thereafter the supernatant liquid was separated from the remaining alkali metal. The volume of the resulting deep yellow solution was reduced to about 30 mL under vacuum, and the obtained precipitate was redissolved by slight warming. Storage at ambient temperature overnight afforded **3** as deep yellow needles. The workup of the mother liquor gave another crop of crystalline material. Yield: 0.826 g (1.29 mmol, 86%); mp: 326–332 °C (minor dec.). ¹H NMR (250.1 MHz, $[D_6]benzene$): δ 0.82 (d, $^3J_{HH} = 6.9$ Hz, 12H, *o*- $CH(CH_3)_2$), 1.05 (d, $^3J_{HH} = 6.9$ Hz, 12H, *p*- $CH(CH_3)_2$), 1.07 (d, $^3J_{HH} = 6.9$ Hz, 12H, *o*- $CH(CH_3)_2$), 2.62 (sep, $^3J_{HH} = 6.9$ Hz, 2H, *p*- $CH(CH_3)_2$), 3.03 (sep, $^3J_{HH} = 6.9$ Hz, 4H, *o*- $CH(CH_3)_2$), 6.89 (s, 4H, *m*-Trip), 7.02 (t, $^3J_{HH} = 7.3$ Hz, 2H, 4- C_6H_4), 7.16 (d, 2H, 3- C_6H_4), 7.39 (t, $^3J_{HH} = 7.3$ Hz, 2H, 5- C_6H_4), 8.38 (d, $^3J_{HH} = 7.3$ Hz, 2H, 6- C_6H_4). ¹³C NMR (62.9 MHz, $[D_6]benzene$): δ 23.9 (*o*- $CH(CH_3)_2$), 24.2 (*o*- $CH(CH_3)_2$), 24.5 (*p*- $CH(CH_3)_2$), 30.6 (*o*- $CH(CH_3)_2$), 34.1 (*p*- $CH(CH_3)_2$), 114.8 (6- C_6H_4), 119.5 (*m*-Trip), 120.5 (4- C_6H_4), 128.9 (5- C_6H_4), 129.3 (3- C_6H_4), 130.7 (2- C_6H_4), 140.9 (*i*-Trip), 147.4 (*p*-Trip), 148.9 (*o*-Trip), 153.2 (1- C_6H_4). IR (Nujol) $\bar{\nu} = 1602$ m, 1584 s, 1561 m, 1481 sh, 1437 s, 1358 s, 1298 vs br, 1228 vs br, 1212 sh, 1195 sh, 1147 ms, 1126 m, 1102 m, 1068 m, 1055 m, 1035 w, 1002 ms, 946 w, 932 m, 898 w, 881 ms, 860 m, 841 w, 822 w, 786 m, 765 sh, 749 vs, 714 ms, 658 ms, 645 m, 593 w, 529 w, 477 m, 450 w. EI MS (70 eV) *m/z* (%): 639.4 (100) [M^+], 573.4 (2) [Tph_2NH]⁺. Anal. Calcd for $C_{42}H_{54}KN_3$: C, 78.82; H, 8.50; N, 6.57. Found: C, 78.20; H, 8.48; N 6.58.

$KN_3(Dmp)Mph$ (2b). The synthesis was accomplished in a manner similar to the preparation of **2a** with use of triazene **1b** (0.55 g, 1.00 mmol). Yield: 0.55 g (0.93 mmol, 93%) as a bright yellow powder; mp: 198–200 °C (dec.). ¹H NMR (400.1 MHz, $[D_6]benzene$): δ 1.81 (s, 6H, *o*- CH_3 Mph), 1.95 (s, 3H, *p*- CH_3 Mph), 2.15 (s, 6H, *p*- CH_3 Dmp), 2.18 (s, 12H, *o*- CH_3 Dmp), 6.43 (s, 2H, *m*-Mes Mph), 6.59 (d, 1H, 6- C_6H_4), 6.75 (s, 4H, *m*-Mes Dmp),

- (20) Tesh, K. F.; Hanusa, T. P.; Huffman, J. C. *Inorg. Chem.* **1990**, *29*, 1584.
 (21) Klinkhammer, K. W.; Henkel, S. J. *Organomet. Chem.* **1994**, *480*, 167.
 (22) Weiss, E. *Helv. Chim. Acta* **1963**, *46*, 2051.
 (23) Dahl, L. F.; Davis, G. L.; Wangler, D. L.; West, R. J. *Inorg. Nucl. Chem.* **1962**, *24*, 357.
 (24) Luger, P.; Andre, C.; Rudert, R.; Zobel, D.; Knochel, A.; Krause, A. *Acta Crystallogr.* **1992**, *B48*, 33.
 (25) For a preliminary report dealing with complexes $[MN_3Tph_2]$ (M = Li, K, Cs) see: (a) Lee, H. S.; Niemeyer, M. *Inorg. Chem.* **2006**, *45*, 6126.
 (26) Hauber, S.-O.; Lissner, F.; Deacon, G. B.; Niemeyer, M. *Angew. Chem.* **2005**, *117*, 6021; *Angew. Chem. Int. Ed.* **2005**, *44*, 5871.
 (27) Niemeyer, M.; Hauber, S.-O. *Inorg. Chem.* **2005**, *44*, 8644.
 (28) Balireddi, S.; Niemeyer, M. *Acta Crystallogr.* **2007**, *E63*, 03525.
 (29) (a) Lüning, U.; Wangnick, C.; Peters, K.; Von Schnering, H. G. *Chem. Ber.* **1991**, *124*, 397. (b) Saednya, A.; Hart, H. *Synthesis* **1996**, 1455. (c) Simons, R. S.; Haubrich, S. T.; Mork, B. V.; Niemeyer, M.; Power, P. P. *Main Group Chem.* **1998**, *2*, 275. (d) von E. Doehring, W.; Dupuy, C. H. *J. Am. Chem. Soc.* **1953**, *75*, 5955. (e) Gavenonis, J.; Tilley, T. D. *Organometallics* **2002**, *21*, 5549.
 (30) (a) Hope, H. *Prog. Inorg. Chem.* **1995**, *41*, 1. (b) *SHELXTL PC 5.03*; Siemens Analytical X-Ray Instruments Inc.: Madison, WI, 1994. (c) Sheldrick, G. M. *Program for Crystal Structure Solution and Refinement*; Universität Göttingen: Göttingen, 1997. (d) van der Sluis, P.; Spek, A. L. *Acta Crystallogr.* **1990**, *A46*, 194. (e) Spek, A. L. *PLATON-98*; Utrecht University: Utrecht, The Netherlands, 1998.

6.92 (dd, 1H, 3-C₆H₄), 6.99 (t, 1H, 4-C₆H₄), 7.07 (m, 3H, C₆H₃), 7.30 (td, 1H, 5-C₆H₄). ¹³C NMR (100.6 MHz, [D₆]benzene): δ 20.9 (*p*-CH₃, Dmp), 21.2 (*o*-CH₃, Dmp), 20.6 (*p*-CH₃, Mph), 21.0 (*o*-CH₃, Mph), 118.7 (6-C₆H₄), 120.6 (4-C₆H₄), 121.6 (5'-C₆H₃), 127.1 (*m*-Mes, Mph), 127.7 (*m*-Mes, Dmp), 127.7 (3-C₆H₄), 128.3 (5-C₆H₄), 129.0 (4'/6'-C₆H₃), 130.8, 132.8, 134.3, 134.7, 136.6, 137.7, 142.1, 142.1 (various aromatic C), 151.0, 153.8 (1-C₆H₄, 2'-C₆H₃). Anal. Calcd for C₃₉H₄₀KN₃: C, 79.41; H, 6.84; N, 7.12. Found: C, 79.29; H, 6.89; N 7.10.

KN₃(Dmp)Tph (2c). The synthesis was accomplished in a manner similar to the preparation of **2a** with use of triazene **1c** (1.27 g, 2.00 mmol). Yield: 1.24 g (1.84 mmol, 92%) as a bright yellow powder; mp: 178–214 °C (dec.). ¹H NMR (400.1 MHz, [D₆]benzene): δ 0.69 (d, ³J_{HH} = 6.9 Hz, 6H, *o*-CH(CH₃)₂), 0.94 (d, ³J_{HH} = 6.9 Hz, 6H, *o*-CH(CH₃)₂), 1.03 (d, ³J_{HH} = 6.9 Hz, 6H, *p*-CH(CH₃)₂), 2.17 (s, 12H, *o*-CH₃), 2.17 (s, 6H, *p*-CH₃), 2.59 (sep, ³J_{HH} = 6.9 Hz, 2H, *p*-CH(CH₃)₂), 2.80 (sep, ³J_{HH} = 6.9 Hz, 1H, *o*-CH(CH₃)₂), 6.52 (dd, 1H, 6-C₆H₄), 6.78 (s, 4H, *m*-Mes), 6.80 (s, 2H, *m*-Trip); 6.96 (td, 1H, 4-C₆H₄), 7.00–7.07 (m, 3H, C₆H₃), 7.03 (dd, 1H, 3-C₆H₄), 7.28 (td, 1H, 5-C₆H₄) ppm. ¹³C NMR (62.9 MHz, [D₆]benzene): δ 21.0 (*p*-CH₃), 21.1 (*o*-CH₃), 23.7 (*o*-CH(CH₃)₂), 24.2 (*o*-CH(CH₃)₂), 24.6 (*p*-CH(CH₃)₂), 30.4 (*o*-CH(CH₃)₂), 34.4 (*p*-CH(CH₃)₂), 117.0 (6-C₆H₄), 119.5 (*m*-Trip), 119.9 (4-C₆H₄), 120.9 (5'-C₆H₃), 127.7 (*m*-Mes), 128.4 (5-C₆H₄), 128.6 (3-C₆H₄), 129.3 (4'/6'-C₆H₃), 129.9 (2-C₆H₄), 131.8 (1'/3'-C₆H₃), 134.7 (*p*-Mes), 136.3 (*o*-Mes), 140.8 (*i*-Trip), 142.9 (*i*-Mes), 147.3 (*p*-Trip), 148.8 (*o*-Trip), 149.8 (2'-C₆H₃), 153.8 (1-C₆H₄) ppm. Anal. Calcd for C₄₅H₅₂KN₃: C, 80.19; H, 7.78; N, 6.23. Found: C, 79.98; H, 7.80; N 6.13.

KN₃(Me₄Ter)₂ (2d). The synthesis was accomplished in a manner similar to the preparation of **2a** with use of triazene **1d** (0.92 g, 1.50 mmol). Yield: 0.78 g (1.20 mmol, 80%) as light yellow crystals; mp: 225–290 °C (changes color to orange and red and decomposes to a red oil). ¹H NMR (250.1 MHz, C₆D₆): δ 1.97 (s, 24H, CH₃), 6.67 (s, 4H, *p*-C₆H₃Me₂), 6.67 (s, 8H, *o*-C₆H₃Me₂), 6.91 (t, ³J_{HH} = 7.5 Hz, 2H, *p*-C₆H₃), 7.13 (d, ³J_{HH} = 7.5 Hz, 4H, *o*-C₆H₃). IR (Nujol) $\bar{\nu}$ = 1599 ms, 1573 sh, 1407 m, 1284 vs br, 1252 sh, 1229 sh, 1215 sh, 1198 s, 1169 m, 1123 w, 1036 m, 948 w, 888 m, 845 vs, 794 ms, 762 s, 751 s, 714 vs, 702 vs, 670 ms, 609 w, 521 w, 508 w, 482 w, 388 m, 340 m, 311 m.

TiN₃Tph₂ (3a). TIOEt (0.125 mL, 1.76 mmol) was added at 0 °C to a stirred solution of **1a** (1.04 g, 1.73 mmol) in 50 mL of an *n*-heptane/toluene (4:1) mixture and stirring was continued for 30 min. The resulting orange suspension was heated to 80 °C, and solid byproducts (mainly Ti metal) were separated by centrifugation. Storage of the obtained solution at ambient temperature overnight afforded **3a** as orange crystals. The workup of the mother liquor gave another crop of crystalline material. Yield: 1.08 g (1.34 mmol, 77%); mp: 289–293 °C (dec.). ¹H NMR (250.1 MHz, [D₆]benzene): δ 1.02 (d, ³J_{HH} = 6.9 Hz, 12H, *o*-CH(CH₃)₂), 1.06 (d, ³J_{HH} = 6.9 Hz, 12H, *o*-CH(CH₃)₂), 1.14 (d, ³J_{HH} = 6.9 Hz, 12H, *p*-CH(CH₃)₂), 2.67 (sep, ³J_{HH} = 6.9 Hz, 2H, *p*-CH(CH₃)₂), 2.90 (sep, ³J_{HH} = 6.9 Hz, 4H, *o*-CH(CH₃)₂), 6.99 (td, ³J_{HH} = 7.2 Hz, ⁴J_{HH} = 1.2 Hz, 2H, 4-C₆H₄), 7.10 (s, 4H, *m*-Trip), 7.09 (dd, ³J_{HH} = 7.33 Hz, ⁴J_{HH} = 1.8 Hz, 2H, 3-C₆H₄), 7.36 (td, ³J_{HH} = 7.3 Hz, ⁴J_{HH} = 1.7 Hz, 2H, 5-C₆H₄), 8.13 (d, ³J_{HH} = 7.3 Hz, 2H, 6-C₆H₄). ¹³C NMR (62.9 MHz, [D₆]benzene, 338 K): δ 24.2 (br, *p*-CH(CH₃)₂), 24.2 (br, *o*-CH(CH₃)₂), 24.4 (*o*-CH(CH₃)₂), 30.7 (*o*-CH(CH₃)₂), 34.5 (*p*-CH(CH₃)₂), 115.7 (6-C₆H₄), 121.7 (br, *m*-Trip), 122.3 (4-C₆H₄), 128.6 (5-C₆H₄), 130.3 (3-C₆H₄), 130.8 (2-C₆H₄), 137.9 (br, *i*-Trip), 148.0 (br, *o*-Trip), 148.1 (br, *p*-Trip), 152.3 (br, 1-C₆H₄). IR (Nujol) $\bar{\nu}$ = 1603 m, 1587 m, 1564 m, 1483 sh, 1359 s, 1344 m, 1300 vs br, 1269 sh, 1248 vs br, 1209 sh, 1168 ms, 1150 ms, 1126 m, 1102

ms, 1068 ms, 1054 ms, 1038 m, 1003 ms, 947 w, 935 m, 920 w, 895 w, 879 ms, 860 m, 841 w, 821 w, 782 w, 751 vs, 714 ms, 655 ms, 646 sh, 624 w, 593 w, 527 w, 477 m. Anal. Calcd for C₄₂H₅₄N₃Ti: C, 62.64; H, 6.76; N, 5.22. Found: C, 62.40; H, 6.82; N 5.25.

TiN₃(Dmp)Mph (3b). The synthesis was accomplished in a manner similar to the preparation of **3a** with use of triazene **1b** (0.79 g, 1.27 mmol) and TIOEt (0.10 mL, 1.42 mmol). Yield: 0.69 g (0.91 mmol, 72%) as orange crystals. ¹H NMR (400.1 MHz, [D₆]benzene): δ 1.85 (s, 6H, *o*-CH₃ Mph), 1.97 (s, 3H, *p*-CH₃ Mph), 2.18 (s, 6H, *p*-CH₃ Dmp), 2.19 (s, 12H, *o*-CH₃ Dmp), 6.53 (d, 1H, 6-C₆H₄), 6.63 (s, 2H, *m*-Mes Mph), 6.87 (s, 4H, *m*-Mes Dmp), 6.88 (dd, 1H, 3-C₆H₄), 6.96 (t, 1H, 4-C₆H₄), 7.03 (m, 3H, C₆H₃), 7.30 (td, 1H, 5-C₆H₄). ¹³C NMR (100.6 MHz, [D₆]benzene): δ 20.7 (*o*-CH₃, Mph), 20.7 (*p*-CH₃, Mph), 21.0 (*p*-CH₃, Dmp), 21.1 (*o*-CH₃, Dmp), 118.2 (6-C₆H₄), 122.2 (4-C₆H₄), 122.9 (5'-C₆H₃), 128.2 (5-C₆H₄), 128.6 (br, *m*-Mes Dmp), 128.7 (3-C₆H₄), 128.9 (br, *m*-Mes Mph), 129.6 (4'/6'-C₆H₃), 130.6, 133.0, 135.8, 136.1 br, 136.2, 136.9, 139.3, 140.4 (various aromatic C), 149.1, 152.2 (1-C₆H₄, 2'-C₆H₃). Anal. Calcd for C₃₉H₄₀TiN₃: C, 62.03; H, 5.34; N, 5.56. Found: C, 62.10; H, 5.38; N 5.53.

TiN₃(Dmp)Tph (2c). The compound was prepared by two different procedures. (a) The first synthesis was accomplished in a manner similar to the preparation of **3a** with use of triazene **1c** (0.95 g, 1.49 mmol) and TIOEt (0.38 g, 1.52 mmol). Yield: 1.02 g (1.22 mmol, 82%) as deep orange crystals. (b) Alternatively, a solution of (thf)₂LiN₃(Dmp)Tph freshly prepared from **1c** (0.636 g, 1.00 mmol) and 2.5 M solution of *n*BuLi (0.40 mL, 1.00 mmol) in 30 mL of thf (40 mL) was added at –20 °C to a suspension of TiCl₄ (0.35 g, 1.46 mmol). Stirring was continued overnight, after which the solvent was removed under reduced pressure. The remaining red-brown solid was extracted with 40 mL of warm *n*-heptane, and solid byproducts were separated by centrifugation. The solution was concentrated and stored at ambient temperature overnight to give **2c** as orange crystalline material (0.66 g, 0.79 mmol, 79%) mp: 198–201 °C. ¹H NMR (400.1 MHz, [D₆]benzene): δ 0.90 (d, ³J_{HH} = 6.9 Hz, 6H, *o*-CH(CH₃)₂), 0.96 (d, ³J_{HH} = 6.9 Hz, 6H, *o*-CH(CH₃)₂), 1.11 (d, ³J_{HH} = 7.0 Hz, 6H, *p*-CH(CH₃)₂), 2.15 (s, 12H, *o*-CH₃), 2.19 (s, 6H, *p*-CH₃), 2.63 (sep, ³J_{HH} = 6.9 Hz, 2H, *p*-CH(CH₃)₂), 2.70 (sep, ³J_{HH} = 6.9 Hz, 1H, *o*-CH(CH₃)₂), 6.52 (dd, 1H, 6-C₆H₄), 6.78 (s, 4H, *m*-Mes), 6.80 (s, 2H, *m*-Trip); 6.96 (td, 1H, 4-C₆H₄), 7.00–7.07 (m, 3H, C₆H₃), 7.03 (dd, 1H, 3-C₆H₄), 7.28 (td, 1H, 5-C₆H₄) ppm. ¹³C NMR (62.9 MHz, [D₆]benzene): δ 20.9 (*o*-CH₃), 21.0 (*p*-CH₃), 24.0 (*p*-CH(CH₃)₂), 24.0 (*o*-CH(CH₃)₂), 24.4 (*o*-CH(CH₃)₂), 30.4 (*o*-CH(CH₃)₂), 34.6 (*p*-CH(CH₃)₂), 117.1 (br, 6-C₆H₄), 121.2 (br, 4-C₆H₄), 121.7 (*m*-Trip), 122.7 (5'-C₆H₃), 128.2 (5-C₆H₄), 128.7 (br, *m*-Mes), 129.5 (3-C₆H₄), 129.8 (4'/6'-C₆H₃), 132.5 (br, 2-C₆H₄), 135.8 (br), 135.9 (br), 140.8 (br, *i*-Trip), 147.9 (br, *o*+*p*-Trip) ppm; four further ¹³C signals could not be detected because of signal overlapping or broadness. IR (Nujol) $\bar{\nu}$ = 1907 w, 1590 m, 1563 m, 1409 m, 1338 m, 1258 vs, 1199 s, 1178 m, 1098 w, 1069 m, 1054 w, 1040 w, 1003 w, 968 w, 946 w, 935 m, 878 m, 865 w, 854 s, 802 m, 788 m, 780 vw, 761 s, 753 s, 378 s, 684 m, 651 w, 645 vw, 587 w, 575 vw, 542 vw, 526 vw, 511 w, 498 vw, 479 vw, 467 vw, 419 w, 403 vw, 394 vw. EI MS (70 eV) *m/z* (%): 839.3 (57.5) [M⁺], 607.3 (4.1) [DmpNTph⁺], 341.1 (5.5) [DmpN₂⁺], 313.1 (33.6) [Dmp⁺], 204.9 (100) [Ti⁺]. Anal. Calcd for C₄₅H₅₂N₃Ti: C, 64.40; H, 6.24; N, 5.01. Found: C, 64.79; H, 6.23; N 5.11.

TiN₃(Me₄Ter)₂ (3d). The synthesis was accomplished in a manner similar to the preparation of **3a** with use of triazene **1d** (0.614 g, 1.00 mmol) and TIOEt (0.274 g, 1.10 mmol). The crude product was recrystallized from an *n*-heptane/benzene (4:1) mixture.

Yield: 0.68 g (0.83 mmol, 83%) as pale yellow crystals; mp: 206–207 °C (dec.; color change to brown). ¹H NMR (250.1 MHz, C₆D₆): δ 2.11 (s, 24H, CH₃), 6.66 (s, 4H, *p*-C₆H₃Me₂), 6.93 (s, 8H, *o*-C₆H₃Me₂), 6.92 (m, 2H, *p*-C₆H₃), 7.21 (d, ³J_{HH} = 7.4 Hz, 4H, *o*-C₆H₃). ¹³C NMR (62.9 MHz, [D₆]benzene): δ 21.4 (CH₃), 122.4 (*p*-C₆H₃), 128.1 (*p*-C₆H₃Me₂), 128.9 (*o*-C₆H₃Me₂), 130.2 (*p*-C₆H₃), 136.3 (*o*-C₆H₃), 136.8 (*m*-C₆H₃Me₂), 143.0 (*i*-C₆H₃Me₂), 149.7 (*i*-C₆H₃) ppm. IR (Nujol) $\bar{\nu}$ = 1601 m, 1455 vs br, 1407 sh, 1335 s, 1279 vs br, 1227 s, 1194 s, 1170 s, 1123 ms, 1079 ms, 1070 sh, 1038 s, 955 m, 905 m, 900 m, 889 s, 882 m, 856 sh, 846 vs, 811 m, 795 s, 783 ms, 762 vs, 751 vs, 712 vs, 702 vs, 683 ms, 670 ms, 643 w, 631 w, 608 w, 543 w, 531 w, 519 w, 504 m, 479 m, 475 sh, 389 vs, 361 ms, 312 m. Anal. Calcd for C₄₄H₄₂N₃Tl: C, 64.67; H, 5.18; N, 5.14. Found: C, 64.49; H, 5.11; N 5.13.

X-ray Crystallography. X-ray-quality crystals were obtained as described in the experimental section. Crystals were removed from Schlenk tubes and immediately covered with a layer of viscous hydrocarbon oil (Paratone N, Exxon). A suitable crystal was selected, attached to a glass fiber, and instantly placed in a low-temperature N₂-stream.^{30a} All data were collected at 173 or 193 K (**2b**) using either a Siemens P4 (**2d**, **2d** (C₅H₁₀)_{1.5}, **3d**), a rebuild Syntex P2₁/Siemens P3 (**2a**, **2c**, **3a–c**) or a Bruker Smart Apex II (**2b**) diffractometer. Crystal data are given in Table 2. Calculations were performed with the SHELXTL PC 5.03^{30b} and SHELXL-97^{30c} program system installed on a local PC. The structures were solved by direct methods and refined on F_o² by full-matrix least-squares refinement. For the thallium complexes, an absorption correction was applied by using semiempirical ψ -scans. Anisotropic thermal parameters were included for all nonhydrogen atoms. In **2a**, the methyl carbon atoms of a disordered isopropyl group were refined with split positions and side occupation factors of 0.67 (C243) and 0.33 (C244). The corresponding C241–C242, C241–C243, and C241–C244 distances were restrained with SADI commands. In **2c**, the methyl carbon atoms of a disordered isopropyl group were refined with split positions and side occupation factors of 0.50 (C442, C444). The corresponding C441–C442, C441–C443, and C441–C444 distances were restrained with DFIX commands. In **2d**, 1.5 additional cyclopentane molecules were located in accessible cavities of the structure. Because they were heavily disordered, their contribution was eliminated from the reflection data using the BYPASS method^{30d} as implemented in the SQUEEZE routine of the PLATON98^{30e} package. In **3a**, the methyl carbon atoms of a disordered isopropyl group were refined with split positions and side occupation factors of 0.75 (C243) and 0.25 (C244). In **3c**, the methyl carbon atoms of one disordered isopropyl group were refined with 0.50 split positions for C442/C444 and C443/C445. The C441–C442, C441–C443, C441–C444, and C441–C445 distances were restrained with DFIX commands. The final *R* values are listed in Table 2. Important bond parameters are given in Figure 6 and in Table 3. Further details are provided in the Supporting Information. Crystallographic data (excluding structure factors) for the structures reported in this paper have been deposited with the Cambridge Crystallographic Data Centre as supplementary publication nos. CCDC-296486 (**2c**), -296487 (**2a**), and -672473 to -672479 (**2b**, **2d**, **2d** (C₅H₁₀)_{1.5}, **3a–3d**). Copies of the data can be obtained free of charge from CCDC, 12 Union Road, Cambridge CB21EZ, U.K. (fax +(44)-1223-336-033; e-mail deposit@ccdc.cam.ac.uk).

Computational Details. The Gaussian 03³¹ package was used for all energy and frequency calculations. The energies of the model compounds were minimized, starting from the crystallographically determined or from other derived geometries, using density functional theory (DFT) with the functionals B3LYP,^{32a–c} MPW1PW91,^{32d} or MPW1B95.^{32e} An energy-consistent, quasi-

relativistic pseudopotential of the Stuttgart/Cologne group with an optimized 12s12p8d3f valence basis set has been employed for the heavier atom thallium (*N* = 60),^{32f} where *N* denotes the number of core-electrons. For the lighter atoms carbon, hydrogen, nitrogen and potassium, the basis sets 6–31G* or 6–31+G* were used. Frequency calculations were done (with 3–21G* basis sets for the lighter atoms) to verify that the geometries are true minima on the potential-energy surface. The natural bond orbital analysis employed the Gaussian 03 adaptation of the NBO program.^{32g} One part of the NBO program, examines all possible interactions between filled (donor) Lewis-type NBOs and empty (acceptor) non-Lewis NBOs and estimates their energetic importance by second-order perturbation theory. The calculated perturbation energy *E*⁽²⁾ corresponds to the associated stabilization by delocalization.

Results and Discussion

Syntheses. The potassium (**2a–d**) and thallium (**3a–d**) triazenides are accessible in *n*-heptane as the solvent via metalation of the diaryltriazenes Tph₂N₃H (**1a**), Dmp(Mph)-N₃H (**1b**), Dmp(Tph)N₃H (**1c**), and (Me₄Ter)₂N₃H (**1d**) (Dmp = 2,6-Mes₂C₆H₃ with Mes = 2,4,6-Me₃C₆H₂; Me₄Ter = 2,6-(3,5-Me₂C₆H₃)₂C₆H₃; Mph = 2-MesC₆H₄; Tph = 2-TripC₆H₄ with Trip = 2,4,6-ⁱPr₃C₆H₂) with either potassium metal or thallium ethoxide (Scheme 1). After crystallization, the complexes [M(N₃Ar₂)] [Ar = Tph (**2a** {M = K}, **3a** {M = Tl}); Ar = Dmp/Mph (**2b**, **3b**); Ar = Dmp/Tph (**2c**, **3c**); Ar = Me₄Ter (**2d**, **3d**)] are isolated in good to excellent yields. The pale yellow (**2d**, **3d**), deep yellow (**2a–2c**), or orange (**3a–3c**) complexes are moisture-sensitive and possess good or moderate solubility in aromatic or aliphatic hydrocarbons. They show considerable thermal stability but decompose with N₂ evolution at higher temperature. The most thermally stable compounds are the Tph derivatives with decomposition ranges as high as 326–332 °C (**2a**) and 289–293 °C (**3a**). The IR spectra show strong ν_{as} N₃ absorptions in the range 1228–1279 cm⁻¹ which is indicative of the triazenido groups acting as chelating ligands.³³

(31) Frisch, M. J.; Trucks, G. W.; Schlegel, H. B.; Scuseria, G. E.; Robb, M. A.; Cheeseman, J. R.; Montgomery, J. A., Jr.; Vreven, T.; Kudin, K. N.; Burant, J. C.; Millam, J. M.; Iyengar, S. S.; Tomasi, J.; Barone, V.; Mennucci, B.; Cossi, M.; Scalmani, G.; Rega, N.; Petersson, G. A.; Nakatsuji, H.; Hada, M.; Ehara, M.; Toyota, K.; Fukuda, R.; Hasegawa, J.; Ishida, M.; Nakajima, T.; Honda, Y.; Kitao, O.; Nakai, H.; Klene, M.; Li, X.; Knox, J. E.; Hratchian, H. P.; Cross, J. B.; Adamo, C.; Jaramillo, J.; Gomperts, R.; Stratmann, R. E.; Yazyev, O.; Austin, A. J.; Cammi, R.; Pomelli, C.; Ochterski, J. W.; Ayala, P. Y.; Morokuma, K.; Voth, G. A.; Salvador, P.; Dannenberg, J. J.; Zakrzewski, V. G.; Dapprich, S.; Daniels, A. D.; Strain, M. C.; Farkas, O.; Malick, D. K.; Rabuck, A. D.; Raghavachari, K.; Foresman, J. B.; Ortiz, J. V.; Cui, Q.; Baboul, A. G.; Clifford, S.; Cioslowski, J.; Stefanov, B. B.; Liu, G.; Liashenko, A.; Piskorz, P.; Komaromi, I.; Martin, R. L.; Fox, D. J.; Keith, T.; Al-Laham, M. A.; Peng, C. Y.; Nanayakkara, A.; Challacombe, M.; Gill, P. M. W.; Johnson, B.; Chen, W.; Wong, M. W.; Gonzalez, C.; Pople, J. A. *Gaussian 03*, Revision D.01; Gaussian, Inc.: Pittsburgh, PA, 2003.

(32) (a) Becke, A. D. *J. Chem. Phys.* **1993**, *98*, 5648. (b) Lee, C.; Yang, W.; Parr, R. G. *Phys. Rev. B* **1988**, *37*, 785. (c) Miehlich, B.; Savin, A.; Stoll, H.; Preuss, H. *Chem. Phys. Lett.* **1989**, *157*, 200. (d) Adamo, C.; Barone, V. *J. Chem. Phys.* **1998**, *108*, 664. (e) Zhao, Y.; Truhlar, D. G. *J. Phys. Chem. A* **2004**, *108*, 6908. (f) Leininger, T.; Berning, A.; Nicklass, A.; Stoll, H.; Werner, H.-J.; Flad, H.-J. *Chem. Phys.* **1997**, *19*, 217. (g) NBO Version 3.1, Glendening, E. D.; Reed, A. E.; Carpenter, J. E.; Weinhold, F. (h) Wiberg, K. B. *Tetrahedron* **1968**, *24*, 1083.

Table 2. Selected Crystallographic Data for Compounds **2a–d** and **3a–d**^a

	2a	3a	2b	3b	2c	3c	2d	3d
formula	C ₄₂ H ₅₄ KN ₃	C ₄₂ H ₅₄ TiN ₃	C ₃₉ H ₄₀ KN ₃	C ₃₉ H ₄₀ TiN ₃	C ₄₅ H ₅₂ KN ₃	C ₄₅ H ₅₂ TiN ₃	C ₄₄ H ₄₂ KN ₃	C ₄₄ H ₄₂ TiN ₃
molecular mass	639.98	805.25	589.84	755.11	674.00	839.27	651.91	817.18
color, habit	yellow, block	orange, prism	yellow, block	orange, prism	yellow, block	orange, prism	light yellow, prism	light yellow, prism
cryst size (mm)	0.75 × 0.75 × 0.35	0.50 × 0.45 × 0.20	0.55 × 0.50 × 0.40	0.45 × 0.35 × 0.30	1.00 × 0.45 × 0.40	0.35 × 0.30 × 0.15	0.60 × 0.50 × 0.30	0.45 × 0.35 × 0.30
cryst syst	triclinic	triclinic	orthorhombic	orthorhombic	triclinic	triclinic	monoclinic	monoclinic
space group	<i>P</i> $\bar{1}$	<i>P</i> $\bar{1}$	<i>P</i> 2 ₁ 2 ₁	<i>P</i> 2 ₁ 2 ₁	<i>P</i> $\bar{1}$	<i>P</i> $\bar{1}$	<i>C</i> 2/ <i>c</i>	<i>C</i> 2/ <i>c</i>
<i>a</i> (Å)	9.4209(14)	9.4318(14)	11.0395(2)	10.9803(19)	9.836(2)	10.033(2)	25.281(5)	27.567(2)
<i>b</i> (Å)	14.406(3)	14.4350(16)	13.4369(2)	13.5172(15)	12.026(3)	12.0160(19)	13.6319(15)	25.457(5)
<i>c</i> (Å)	14.624(3)	14.8042(15)	22.4426(4)	22.695(3)	18.132(4)	18.186(3)	24.677(4)	13.4261(19)
α (deg)	101.089(16)	101.603(8)	90	90	74.59(2)	97.356(12)	90	90
β (deg)	104.113(13)	104.350(10)	90	90	74.69(2)	105.257(14)	90	90
γ (deg)	91.023(14)	90.816(11)	90	90	73.39(2)	107.564(14)	90	90
<i>V</i> (Å ³)	1884.5(6)	1908.4(4)	3329.07(12)	3368.5(8)	1939.9(8)	1964.6(6)	7440(2)	7439(2)
<i>Z</i>	2	2	4	4	2	2	8	8
<i>d</i> _{calc} (g/cm ³)	1.128	1.401	1.177	1.489	1.154	1.419	1.164	1.459
μ (mm ⁻¹)	0.173	4.263	0.190	4.825	0.171	4.144	0.176	4.376
2θ range (deg)	3–55	4–56	3–56	4–56	4–54	4–55	4–50	4–54
collected data	9154	9757	62270	5578	8984	9560	6693	8289
unique data/ <i>R</i> _{int}	8625/0.019	9211/0.024	7968/0.071	5316/0.023	8478/0.029	9011/0.023	6533/0.094	8405/0.056
data with <i>I</i> > 2 σ (<i>I</i>) (<i>N</i> _o)	7499	8042	5963	4661	6894	7678	2913	5371
no. of params (<i>N</i> _p)	441	440	399	399	467	479	444	444
no. of restraints	3	0	0	0	4	4	0	0
<i>R</i> 1 (<i>I</i> > 2 σ (<i>I</i>)) ^b	0.052	0.033	0.035	0.035	0.054	0.047	0.040	0.032
<i>wR</i> 2 (all data) ^c	0.146	0.078	0.083	0.080	0.152	0.121	0.088	0.076
GOF ^d	1.028	1.243	0.942	1.147	1.058	1.190	0.697	0.858
resd dens (e/Å ³)	0.52/–0.60	1.00/–1.03	0.16/–0.21	1.21/–0.97	0.59/–0.63	1.95/–2.50	0.19/–0.18	1.12/–1.22

^a All data were collected at 173 or 193 K (**2b**), using Mo K α (= 0.71073 Å) radiation. ^b *R*1 = $\Sigma(|F_o| - |F_c|)/\Sigma(F_o)$. ^c *wR*2 = $\{\Sigma[w(F_o^2 - F_c^2)]/\Sigma(F_o^2)\}^{1/2}$. ^d GOF = $\{\Sigma[w(F_o^2 - F_c^2)]/\Sigma(F_o^2)\}^{1/2}$. ^e Values in brackets refer to the refinement that omits contributions from the solvent (see experimental part).

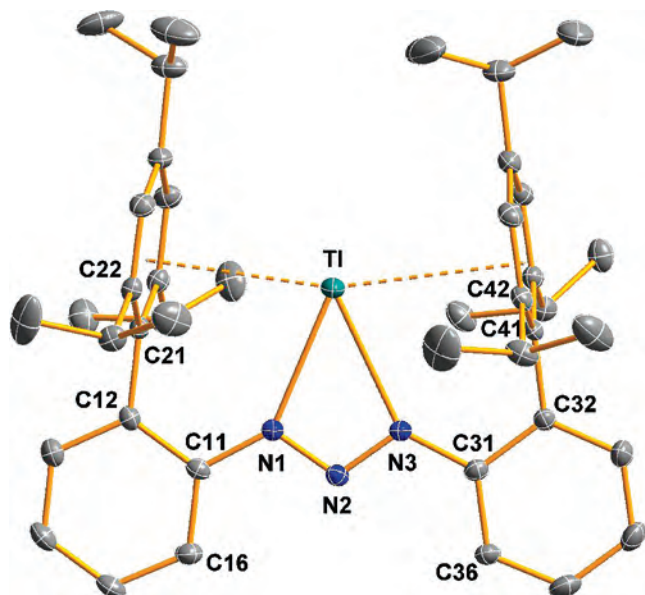


Figure 1. Molecular structure of **3a** with thermal ellipsoids set to 30% probability. Hydrogen atoms have been omitted for clarity.

Structural Studies. All compounds were examined by X-ray crystallography and their molecular structures and important bond parameters are shown in Figures 2–5, and Table 3. Structurally characterized alkali metal triazenides are scarce and have been limited so far to two solvated species with tolyl substituents, a dimeric lithium, and a polymeric potassium complex.^{34a} Very recently, the synthesis and structural characterization of an unsolvated polymeric potassium triazenide was reported.^{34b} Structurally authenticated thallium(I) triazenides are limited to two dimeric complexes.³⁵

MN₃Tph₂ Complexes. Deep yellow crystals of **2a** and orange crystals of **3a**, suitable for X-ray crystallographic studies, were grown from a saturated C₆D₆ solution at ambient temperature. Both compounds crystallize with isomorphous cells in the triclinic space group *P* $\bar{1}$. Figure 1 shows a representation of the Tl complex. The size of the η^2 -bonded triazenide ligands enforces the formation of strictly monomeric compounds in which the metal cations possess apparent low coordination numbers of 2. With a range of 1.301(4)–1.3086(17) Å, the N–N distances within the triazenido ligand cores are consistent with delocalized bonding. The coordination of the triazenide ligands is rather symmetrical with little variation of the K–N [average 2.716(1) Å] and Tl–N [average 2.593(3) Å] bond lengths. The former distances are considerably shorter than those in the polymeric complexes [$\{ \text{KN}_3\text{Tol}_2(\text{dme}) \}_2$]_∞ (Tol = 4-MeC₆H₄; av. 2.886 Å)^{34a} and [$\{ \text{KN}_3(4\text{-NO}_2\text{C}_6\text{H}_4)_2 \}_2$]_∞ (av. 2.944 Å),^{34b} which contain 7- and 8-coordinate metal atoms, respectively. In agreement with the higher coordination

number of 3–4, neglecting any additional Tl⋯O, Tl⋯Tl, and Tl⋯arene contacts, longer Tl–N distances than those in **3a** are observed in the dimeric complexes [$\{ \text{TlN}_3\text{Ph}_2 \}_2$] (2.615–3.031 Å, av. 2.78 Å)^{35a} and [$\{ \text{TlN}_3(4\text{-NO}_2\text{C}_6\text{H}_4)_2 \}_2$] (2.934–3.031 Å, av. 2.92 Å).^{35b} However, significantly shorter Tl–N bond lengths have been reported for monomeric low-coordinate thallium(I) amides (cn_{Tl} = 1, plus additional Tl⋯arene contacts, 2.348–2.379 Å),³⁶ β -diketimines (cn_{Tl} = 2, 2.403–2.471 Å),³⁷ and amidinates (cn_{Tl} = 1, plus additional Tl⋯arene contacts, 2.445 Å).³⁸ The longer distances in **3a** are most likely a result of the decreased donor ability of the triazenide relative to the closely related amidinate and β -diketiminato ligands as discussed below and/or a consequence of the additional metal– π -arene interactions.

Besides their monomeric nature, the most interesting feature in the solid-state structures of **2a** and **3a** is the presence of additional metal⋯ π -arene contacts to the flanking aryl groups that provide steric and electronic saturation of the metal cations. In **2a**, the metal ion interacts with the Trip rings of the biphenyl substituents in a η^6/η^5 fashion with K⋯C distances in the range 3.2948(17)–3.3689(17) Å (C21→C26) and 3.3060(17)–3.4482(18) Å (C41, C42, C44→C46). The propensity of potassium to interact with aromatic groups is now well documented.³⁹ The mean K⋯centroid distance of 3.06 Å to the π -bonded Trip arene rings is unexceptional.⁴⁰

It should be noted that the assignment of the hapticity of the metal– π -arene interactions in the compounds discussed in this paper is based on the evaluation of the shortest metal⋯centroid separation. Alternatively, the smallest angle between the M⋯centroid vector and the normal of the arene plane may be used to determine the best description. To allow a better comparison Table 3 not only shows the assigned M⋯centroid (X_n/X_m) distances but also the distances to the center ($X6/X6'$) of the coordinated arene rings. In **3a**, the thallium⋯ π -arene interactions are best described as being η^5/η^5 . The Tl⋯C distances considered to be bonding are in the range 3.299(3)–3.493(3) Å (C21→C23, C25, C26) and 3.373(3)–3.564(3) Å (C41→C43, C45, C46) with corresponding Tl⋯centroid ($X6/X6'$) separations of 3.13 Å and 3.20 Å, respectively. The latter fall within the typical range of Tl⋯centroid distances (2.85–3.18 Å)⁴¹ observed for other structurally characterized Tl– π -arene complexes.⁴² The

(33) Moore, D. S.; Robinson, S. D. *Adv. Inorg. Chem. Radiochem.* **1986**, *30*, 1.

(34) (a) Gantzel, P.; Walsh, P. J. *Inorg. Chem.* **1998**, *37*, 3450. (b) Hörner, M.; da Silva, A. M.; Fenner, H. *Z. Anorg. Allg. Chem.* **2007**, *633*, 776.

(35) (a) Beck, J.; Strähle, J. Z. *Naturforsch.* **1986**, *41b*, 1381. (b) Hörner, M.; de Oliveira, G. M.; Bresolin, L.; de Oliveira, A. B. *Inorg. Chim. Acta* **2006**, *359*, 4631.

(36) Wright, R. J.; Brynda, M.; Power, P. P. *Inorg. Chem.* **2005**, *44*, 3368.

(37) (a) Cheng, Y.; Hitchcock, P. B.; Lappert, M. F.; Zhou, M. *Chem. Commun.* **2005**, 752. (b) Hill, M. S.; Hitchcock, P. B.; Pongtavorn-pinyo, R. *Dalton Trans.* **2005**, 273.

(38) Jones, C.; Junk, P. C.; Platts, J. A.; Rathmann, D.; Stasch, A. *Dalton Trans.* **2005**, 2497.

(39) Smith, J. D. *Adv. Organomet. Chem.* **1999**, *43*, 354.

(40) (a) For other compounds that show interactions between potassium cations and arene rings of Trip substituents, see the following references. Herein, the K⋯centroid distances fall in the range 2.74–3.19 Å. Grisby, W. J.; Power, P. P. *J. Am. Chem. Soc.* **1996**, *118*, 7981. (b) Niemeyer, M.; Power, P. P. *Inorg. Chem.* **1996**, *35*, 7264. (c) Niemeyer, M.; Power, P. P. *Inorg. Chim. Acta.* **1997**, *263*, 201. (d) Pu, L.; Phillips, A. D.; Richards, A. F.; Stender, M.; Simons, R. S.; Olmstead, M. M.; Power, P. P. *J. Am. Chem. Soc.* **2003**, *125*, 11626.

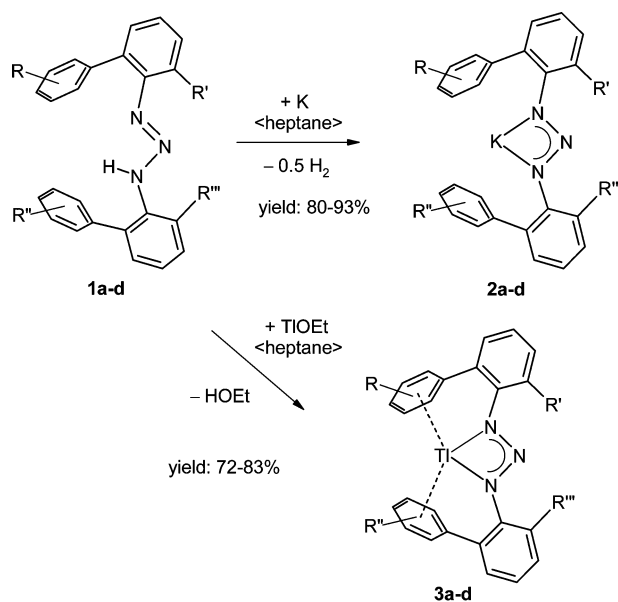
(41) Cambridge Structural Database, London, U.K., 2007. For the search, the range of the Tl⋯centroid–C angles was constrained to 85°–95°, assuming only small ring slippage. For a larger ring slippage, there appears to be no upper limit to the Tl⋯centroid distances.

Table 3. Selected Bond Distances (Å), Angles (deg), and Dihedral Angles (deg) for Compounds **2a**, **3a**, **2b**, **3b**, **2c**, and **3c**^{a,b}

	2a	3a	2b	3b	2c	3c
M-N1	2.7093(14)	2.578(3)	2.7657(13)	2.669(5)	2.7420(17)	2.638(4)
M-N3	2.7232(14) {2.716}	2.607(3) {2.593}	2.6574(13) {2.712}	2.546(5) {2.608}	2.6704(16) {2.706}	2.525(4) {2.582}
M...N2	3.2467(13)	3.115(3)	3.2347(13)	3.125(5)	3.2104(17)	3.083(4)
N1–N2	1.3016(18)	1.301(4)	1.3041(17)	1.311(7)	1.308(2)	1.287(6)
N2–N3	1.3086(17)	1.301(4)	1.3155(17)	1.314(6)	1.316(2)	1.312(6)
M...C21	3.3166(16)	3.299(3)	3.3783(16)	3.374(7)	3.343(2)	3.390(5)
M...C22	3.3472(16)	3.371(3)	3.4038(16)	3.466(6)	3.296(2)	3.414(5)
M...C23	3.3636(17)	3.493(3)	3.3773(17)	3.525(6)	3.280(2)	3.474(6)
M...C24	3.3689(17)	3.569(3)	3.3508(18)	3.533(7)	3.339(2)	3.509(6)
M...C25	3.3074(18)	3.477(4)	3.3156(18)	3.427(7)	3.372(2)	3.493(6)
M...C26	3.2948(17) {3.333}	3.351(3) {3.427}	3.3462(18) {3.362}	3.371(7) {3.449}	3.396(2) {3.338}	3.437(6) {3.453}
M...C41	3.3583(16)	3.373(3)	3.3054(16)	3.289(6)	3.322(2)	3.293(5)
M...C42	3.4435(17)	3.454(3)	3.4149(17)	3.447(6)	3.359(2)	3.336(5)
M...C43	3.4759(18)	3.564(3)	3.3834(18)	3.527(7)	3.370(2)	3.479(6)
M...C44	3.4482(18)	3.614(3)	3.2955(17)	3.481(7)	3.375(2)	3.593(6)
M...C45	3.3359(18)	3.519(3)	3.2195(18)	3.350(7)	3.339(3)	3.549(6)
M...C46	3.3060(17) {3.395}	3.412(3) {3.489}	3.2317(18) {3.308}	3.273(7) {3.395}	3.335(2) {3.350}	3.414(5) {3.444}
η^n/η^m	η^6/η^5	η^5/η^5	η^6/η^5	η^5/η^5	η^6/η^6	η^5/η^4
M...X6/M...Xn	3.027	3.131/3.114	3.059	3.159/3.153	3.033	3.160/3.158
M...X6'/M...Xm	3.095/3.088	3.198/3.185	3.000/2.994	3.097/3.080	3.046	3.151/3.129
X6...M...X6'	159.7	154.0	137.6	138.8	140.9	134.4
N2–N1–C11–C16	3.7(2)	2.2(5)	33.7(2)	30.2(10)	–42.5(3)	–41.3(7)
N2–N3–C31–C36	–4.4(2)	–4.9(5)	–20.7(2)	–21.1(9)	19.7(3)	17.2(7)

^a Average values are given in braces. ^b Centroids of the C21→C26 (X6) and C41→C46 (X6') rings.

Scheme 1. Synthesis of Compounds **2a–d** and **3a–d**



1a, **2a**, **3a**: R = R' = 2,4,6-*i*Pr₃, R' = R''' = H

1b, **2b**, **3b**: R = R' = 2,4,6-Me₃, R' = 2,4,6-Me₃C₆H₂, R''' = H

1c, **2c**, **3c**: R = 2,4,6-Me₃, R' = 2,4,6-Me₃C₆H₂, R'' = 2,4,6-*i*Pr₃, R''' = H

1d, **2d**, **3d**: R = R' = 3,5-Me₂, R' = R''' = 3,5-Me₂C₆H₃

shortest Ti...arene separations are found in compounds with weakly coordinating anions and electron-rich aromatic rings such as [Ti(η^6 -MesH)₂][B(OTeF₅)₄].^{42b}

For **2a** and **3a**, the coplanar arrangement of the C₆H₄ rings with the NNN plane, as indicated by the dihedral angles N2–N1–C11–C16 [**2a**: 3.7(2)°; **3a**: 2.2(5)°] and N2–N3–C31–C36 [**2a**: –4.4(2)°; **3a**: –4.9(5)°], together with the perpendicular orientation of the Trip substituents results in a unusual T-shape environment of the metal cations defined by the centroids of the coordinated arene rings and N2 of the triazenido ligand. The absence of particular short intermolecular M...C contacts (**2a**: K...C >5.3 Å; **3a**:

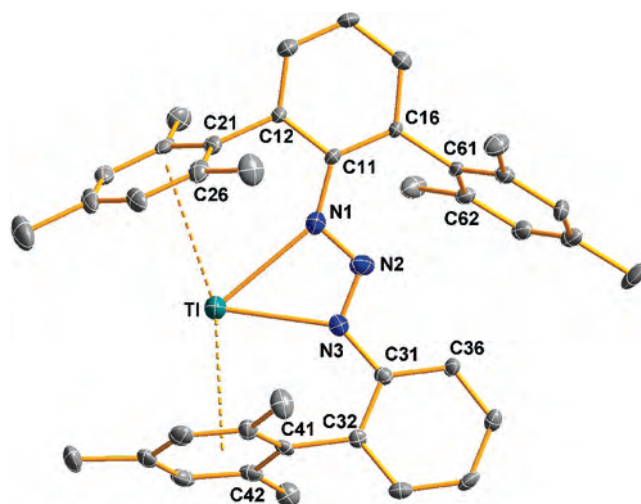


Figure 2. Molecular structure of **3b** with thermal ellipsoids set to 30% probability. Hydrogen atoms have been omitted for clarity.



Figure 3. Space-filling models of **2a** (left), **2b** (middle), and **2c** (right).

Ti...C >5.1 Å) and Ti...Ti contacts (>9.0 Å) supports the monomeric nature for both compounds in the solid-state.

MN₃(Dmp)Mph Complexes. Yellow **2b** and orange **3b** crystallize with very similar cell dimensions in the orthorhombic space group *P*2₁2₁2₁. Figure 2 shows the molecular structure of the thallium complex **3b**. The η^2 -bonded triazenido ligands show slightly asymmetric coordination (**2b**: K–N1 2.7657(13) Å, K–N3 2.6574(13) Å; **3b**: Ti–N1 2.669(5) Å, Ti–N3 2.546(5) Å), with shorter bonds to the biphenyl substituted nitrogen atom. The different steric properties of the biphenyl- and *m*-terphenyl substituents give

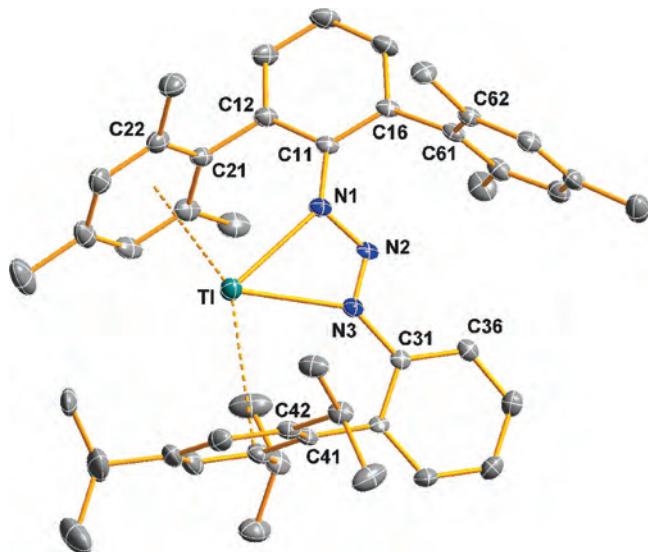


Figure 4. Molecular structure of **3c** with thermal ellipsoids set to 30% probability. Hydrogen atoms have been omitted for clarity.

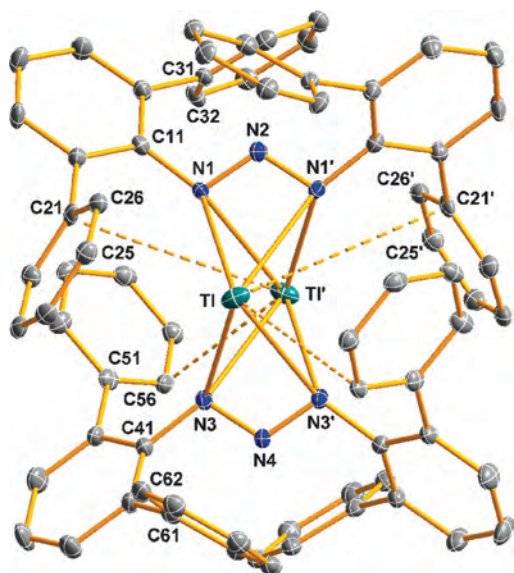


Figure 5. Molecular structure of **3d** with thermal ellipsoids set to 30% probability. Hydrogen atoms and methyl carbon atoms have been omitted for clarity. Selected bond lengths, intermolecular contacts (Å), and dihedral angles (deg) for **3d** and **2d** (in braces): M–N1 = 2.781(3) {2.857(2)}, M–N3 = 2.779(3) {2.874(2)}, M–N1' = 2.915(3) {2.909(2)}, M–N3' = 2.883(3) {2.895(2)}, M···N2 = 3.204(4) {3.249(3)}, M···N4 = 3.190(4) {3.254(3)}, M···C21 = 3.463(4) {3.563(3)}, M···C25 = 3.533(4) {3.458(3)}, M···C26 = 3.262(4) {3.224(3)}, M···C56' = 3.282(4) {3.203(3)}, M···M = 3.4886(6) {3.4130(13)}, N2–N1–C11–C16 = 51.4(5) {49.8(3)}, N4–N3–C41–C46 = 50.6(5) {50.4(3)}; [symmetry operation ('): $-x, y, 0.5 - z$].

rise to a different conformation with respect to the central N₃ plane. The C₆H₄ ring of the biphenyl moiety adopts a roughly coplanar arrangement (N2–N3–C31–C36 –20.7(2) [**2b**], –21.1(9) [**3b**]), whereas the central C₆H₃ plane of the terphenyl substituent is significantly more tilted (N2–N1–C11–C16 33.7(2) [**2b**], 30.2(10) [**3b**]) to minimize repulsive interactions between N2 and one of the Mes rings (C61→C66). As a result, the centroids of the flanking Mes ring of the biphenyl substituent (C41→C46) and the second Mes ring of the terphenyl group (C21→C26) lie above the MN₃ plane and coordinate in a η^6/η^5 (**2b**) or η^5/η^5 (**3b**) fashion with

M···C distances considered to be bonding in the range 3.280(2)–3.392(2) Å (**2b**: C21→C26; C41; C43→C46) and 3.3217(19)–3.396(2) Å (**3b**: C21; C22; C24→C26; C41; C42; C44→C46), respectively. The resulting rather distorted trigonal-pyramidal coordination is reflected by the angles N2···M–X6/X6' (**2b**: 94.7°/100.8°; **3b**: 97.2°/103.5°) and X6–M–X6' (**2b**: 137.6°; **3b**: 138.8°), where X6 and X6' define the centroids of the coordinated arene rings and the bidentate triazenido ligand occupies only one coordination site.

The biggest difference in the solid-state structures of **2a** and **3a** on one side and **2b** and **3b** on the other side involves the orientation of the coordinated arene rings with respect to the central NNN plane. In **2a** and **3a** a perpendicular orientation with dihedral angles in the range 86.9°–93.3° is observed, which leads to perfectly shielded metal cations. In contrast, the corresponding dihedral angles for **2b** and **3b** are found in the range 72.0°–119.5°. As a result, the metal cations are less shielded (Figure 3) and accessible for additional intermolecular and relatively short η^1 - π -arene contacts (M···C34': 3.052 Å [**2b**], 3.200 Å [**3b**]; symmetry operation: $0.5 + x, 1.5 - y, 2 - z$).

MN₃(Dmp)Tph Complexes. Again, the bright yellow potassium compound **2c** and the orange thallium derivative **3c** crystallize with closely related cells in the triclinic space group $P\bar{1}$. Figure 4 shows the molecular structure of the thallium complex **3c**. The average M–N distances of 2.706 Å [**2c**] or 2.582 Å [**3c**] to the slightly asymmetric η^2 -coordinate triazenide ligand are very close to the corresponding values in the previously discussed compounds. Additional metal··· π -arene are observed to one Mes ring (C21→C26) of the terphenyl substituent and the Trip ring (C41→C46) of the flanking biaryl group. For the potassium complex, almost perfect η^6/η^6 coordination is observed with K···C distances spanning the relatively narrow range of 3.280(2)–3.396(17) Å and almost identical K···centroid separations. On the basis of the shortest metal···centroid separation, the arene coordination for the thallium complex is best described as being η^5/η^4 with TI···C distances considered to be bonding in the range of 3.293(5)–3.493(6) Å. Taking the centroids X6 and X6' of the π -bonded arene rings and N2 of the triazenide ligand as reference points, the coordination of the metal atoms may be regarded as distorted trigonal-pyramidal as shown by the angles N2···M–X6/X6' (**2c**: 94.7°/101.1°; **3c**: 95.3°/104.6°) and X6–M–X6' (**2c**: 140.9°; **3c**: 134.4°).

Because of the different steric properties of the Tph and Dmp substituents and interligand repulsion, the torsion angles

- (42) (a) See for example refs 10, 14e, 35a and Schmidbauer, H.; Bublak, W.; Riede, J.; Müller, G. *Angew. Chem., Int. Ed. Engl.* **1985**, *24*, 414. (b) Noirot, M. D.; Anderson, O. P.; Strauss, S. H. *Inorg. Chem.* **1987**, *26*, 2216. (c) Schmidbauer, H.; Bublak, B.; Huber, B.; Hoffmann, J.; Müller, G. *Chem. Ber.* **1989**, *122*, 265. (d) Waezsada, S. D.; Belgardt, T.; Noltemeyer, M.; Roesky, H. W. *Angew. Chem., Int. Ed. Engl.* **1994**, *33*, 1351. (e) Frank, W.; Korrell, G.; Reiss, G. *J. Z. Anorg. Allg. Chem.* **1995**, *621*, 765. (f) Frank, W.; Korrell, G.; Reiss, G. *J. Organomet. Chem.* **1996**, *506*, 293. (g) Kunrath, F. A.; Casagrande, O. L.; Toupet, L.; Carpentier, J.-F. *Eur. J. Inorg. Chem.* **2004**, 4803. (h) Oberbeckmann-Winter, N.; Braunstein, P.; Welter, R. *Organometallics* **2004**, *23*, 6311. (i) Thomas, J. C.; Peters, J. C. *Polyhedron* **2004**, *23*, 2901. (j) Dias, H. V. R.; Singh, S.; Cundari, T. R. *Angew. Chem., Int. Ed.* **2005**, *44*, 4907.

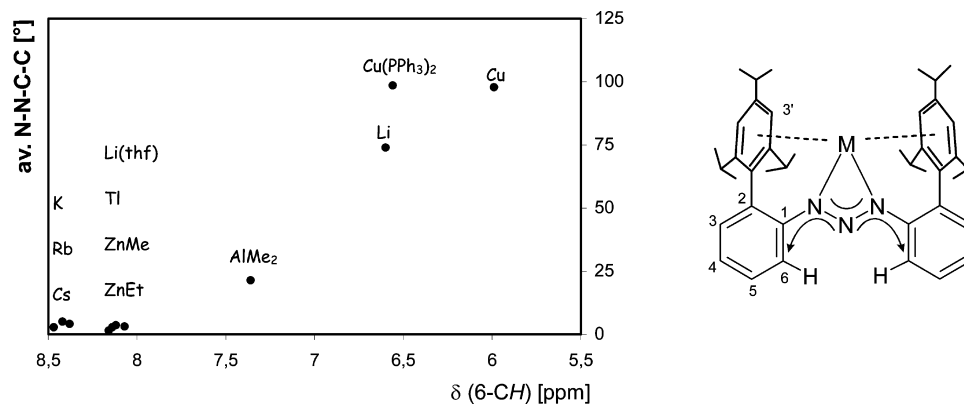


Figure 6. Correlation between the chemical shift $\delta(6\text{-CH})$ (in solution) and the average N–N–C–C torsion angle, taken from the solid-state structures, for a series of metal salts MN_3Tph_2 .^{25,43}

$\text{N}2\text{--N}3\text{--C}31\text{--C}36$ and $\text{N}2\text{--N}1\text{--C}11\text{--C}16$ differ by approximately 25° . As a consequence, the orientation of the coordinated arene rings to the central NNN plane in **2c** and **3c** is close to orthogonal for the $\text{C}41\text{--C}46$ rings of the biphenyl substituents but deviates considerably from orthogonality for the $\text{C}21\text{--C}26$ rings of the terphenyl substituents as indicated by the dihedral angles of $81.5^\circ/82.8^\circ$ (**2c/3c**) and $61.6^\circ/59.2^\circ$ (**2c/3c**), respectively. This orientation leaves room for two additional agostic interactions (**2c**: 3.872 Å and 3.907 Å; **3b**: 3.916 Å and 4.114 Å) from the metal cations to methyl carbon atoms of neighbor molecules. The intermolecular interactions are much weaker than those in **2b** and **3b** because of the larger size of the Tph compared to the Mph substituent and the better shielding of the metal atoms by the former (Figure 3).

$\text{MN}_3(\text{Me}_4\text{Ter})_2$ Complexes. Pale yellow crystals of **2d** and **3d**, suitable for X-ray crystallographic studies, were grown from saturated *n*-heptane/benzene mixtures at ambient temperature. Both compounds crystallize in isomorphous cells with dimeric units in which the metal atoms are bridged by chelating triazenide ligands (Figure 5). Notably, crystallization of the potassium complex **2d** from a cyclopentane/toluene mixture at -20°C affords the solvate **2d** (C_5H_{10})_{1.5}. This complex crystallizes without imposed symmetry with additional solvent molecules located in cavities of the structure (for details, see Supporting Information). The dimeric units in solvent-free **2d** and **3d** contain a 2-fold axis which runs through the central nitrogen atoms of the triazenide ligands and the middle of the $\text{M}\cdots\text{M}'$ vector. In contrast to the previously reported dimeric thallium triazenides,³⁵ which are further aggregated by secondary $\text{Tl}\cdots\text{arene}$ interactions, the dimers in **3d** are strictly isolated, the shortest intermolecular $\text{Tl}\cdots\text{C}$ and $\text{Tl}\cdots\text{Tl}$ contacts being >6.8 Å and >10.7 Å, respectively. Each thallium atom is coordinated to four nitrogen atoms of the bridging triazenide ligands by two shorter ($\text{Tl--N}1 = 2.781(3)$ Å, $\text{Tl--N}3 = 2.779(3)$ Å) and two longer ($\text{Tl--N}1' = 2.915(3)$ Å, $\text{Tl--N}3' = 2.883(3)$ Å) Tl--N separations. The average Tl--N bond distance of 2.840 Å is significant longer than that of the parent complex [$\{\text{TlN}_3\text{Ph}_2\}_2$] (av. 2.78 Å)^{35a} and therefore indicates steric crowding. With a maximum hapticity of three and $\text{Tl}\cdots\text{C}$ separations in the range 3.262(4)–3.533(4) Å, the additional $\text{Tl}\cdots\eta^1\text{-arene}$ (to $\text{C}56'$) and $\text{Tl}\cdots\eta^3\text{-arene}$ (to $\text{C}21$, $\text{C}25$, $\text{C}26$)

interactions are much weaker than those present in **3a–c**. The lower hapticity originates from repulsive forces at the NNN backbone between the $\text{C}31\text{--C}36$ and the $\text{C}31'\text{--C}36'$ rings in one triazenide ligand and the $\text{C}61\text{--C}66$ and the $\text{C}61'\text{--C}66'$ rings in the other. Because of these interactions, a coplanar arrangement of the NNN and C_6H_3 planes is made impossible, and NNCC torsion angles around 51° are observed. As a consequence, a closer approach of arene rings $\text{C}21\text{--C}26$, $\text{C}21'\text{--C}26'$, $\text{C}51\text{--C}56$, and $\text{C}51'\text{--C}56'$ to the two metal centers is prohibited.

In dimeric **2d**, the K--N distances range from 2.857(2) to 2.909(2) Å. The average value of 2.884 Å for the 4-coordinate metal atoms (neglecting additional π -contacts) indicates steric crowding, as in **3d**, since it is almost identical to the mean K--N separation in the solvated polymeric complex [$\{\text{KN}_3\text{ToI}_2(\text{dme})\}_2$]_∞ (av. 2.886 Å),^{34a} which contains a seven-coordinate metal atom. Again, strong π -coordination by the pending 3,5- $\text{Me}_2\text{C}_6\text{H}_3$ rings is prohibited by the noncoplanar conformation of the NNN and C_6H_4 planes with NNCC dihedral angles close to 50° . However, two weak $\eta^1\text{-arene}$ interactions are observed with $\text{K}\cdots\text{C}$ separations of 3.224(3) Å (to $\text{C}26$) and 3.203(3) Å (to $\text{C}56'$).

Solid-State Aggregation Behavior. The different ligand-depending aggregation behavior of complexes **2a–d** and **3a–d** deserves a comment. The degree of aggregation x for $(\text{ML})_x$ compounds (M = monovalent metal, L = monoanionic ligand) depends on a number of factors including the nature of the metal (ionic radius, polarizability), steric demand and hapticity of the substituents, and donor solvation of the metal atom. In homoleptic complexes, higher aggregated derivatives are normally obtained with decreasing steric size of the ligand. Although it is difficult to quantify the steric demand of deprotonated **1a–d**, because of their conformational flexibility/variability, it can be assumed that the size increases in the order $\mathbf{1a} < \mathbf{1b} < \mathbf{1c} < \mathbf{1d}$ and therefore the degree of aggregation for **2a–d** and **3a–d** should decrease in the same direction. However, in the experimentally determined solid-state structures, monomeric (**2a**, **3a**), weakly associated, quasi-monomeric (**2b**, **3b**, **2c**, **3c**), and dimeric (**2d**, **3d**) units with additional metal- η^n - π -arene-interactions of decreasing hapticity n are observed. As explained before, these changes in hapticity arise from different intramolecular repulsive interactions between the

flanking biphenyl or terphenyl groups and are therefore responsible for the “inverse aggregation” behavior.

NMR-Spectroscopic Characterization. The chemical shift for the 6-H atom in the 2-Trip-C₆H₄ substituents of **2a** and **3a** appears to be very sensitive to conformational changes (Figure 6). ¹H NMR studies, in C₆D₆ as the solvent, for a series of metal derivatives MN₃Tph₂ of deprotonated ligand **1a** show a correlation between the chemical shift of this hydrogen atom and the average torsion angle N–N–Cn1–Cn6 (*n* = 1, 3) observed in the solid-state structures.²⁵ A low-field shift in the range 8.07–8.47 ppm consistent with a coplanar *syn/syn* conformation is found for the monomeric complexes with M = K (δ = 8.38), Rb, Cs, Tl (δ = 8.13), Li(thf), ZnMe, ZnEt. Here, either none or only one small additional ligand is present, which fits into the pocket between the flanking arene rings. A third ligand [M = AlMe₂, Cu(PPh₃)₂] or the formation of dimers (M = Li, Cu) leads to steric crowding, larger NNCC dihedral angles, and preference of the *syn/anti* conformation, which is accompanied by a considerable high-field shift up to 5.99 ppm for the *ortho*-H atom. The upfield shift in the *syn/anti* conformers may be explained by ring current effects, whereas the deshielding in the *syn/syn* forms is due to the formation of weak C–H \cdots N hydrogen bridges. We therefore conclude that the conformation of **2a** and **3a** must be similar to that in the solid-state and that the π -encapsulation of the metal cations is retained in solution. In the case of the mixed biphenyl and terphenyl substituted potassium and thallium triazenides **2b**, **2c**, **3b**, and **3c**, the chemical shift for the 6-H atom in the 2-Mes-C₆H₄ or 2-Trip-C₆H₄ substituents is found in the range 6.52–6.59 ppm. According to Figure 6 this would be consistent with an average N2–N3–C31–C36 torsion angle of about 75° which is much higher than the experimentally observed values of approximately $\pm 20^\circ$ in the solid-state structures. However, the higher shielding may be explained by additional ring current effects because the 6-H atom in the 2-Mes-C₆H₄ or 2-Trip-C₆H₄ biphenyl substituents points toward the center of the C61→C66 Mes ring of the 2,6-Mes₂-C₆H₃ terphenyl substituent. Similar trends as in the ¹H NMR spectra, however with opposite sign, are observed for the resonances of the 6-C atoms in the ¹³C NMR spectra. Here, the signals for compounds **2a** and **3a** are shifted to higher field at 114.8 ppm and 115.7 ppm, respectively, whereas the corresponding chemical shifts for **2b**, **2c**, **3b**, and **3c** are found in the range 117.0–118.7 ppm.

DFT Calculations. To further understand the bonding situation in the potassium triazenides **2a–c** with weaker K–N but stronger K \cdots arene bonding on one side and the thallium triazenides **3a–c** with relatively stronger Tl–N but weaker Tl \cdots arene bonding on the other side, DFT calculations were undertaken. However, keeping in mind that these methods are known to be poor at describing weak interactions that are important in noncovalent bonding, such as the London dispersion (van der Waals attraction), dipole–dipole interaction, or hydrogen bonding, we have used not only

Table 4. Selected Experimental and DFT-Calculated Bond Distances (Å), Angles (deg), and Dihedral Angles (deg) for Compounds **2a**, **3a**

	2a {3a}	2a {3a}	2a {3a}	2a {3a}	2a {3a}
	exp	b3lyp	mpw1pw91	mpw1b95	mpw1b95
		6–31G*	6–31G*	6–31G*	6–31+G*
av. M–N	2.716	2.712	2.701	2.729	2.730
	2.593	2.603	2.585	2.605	2.613
av. N–N	1.305	1.305	1.297	1.294	1.293
	1.301	1.300	1.292	1.288	1.288
av. M \cdots C	3.364	3.549	3.500	3.285	3.334
	3.458	3.753	3.638	3.511	3.518
M \cdots X6	3.061	3.259	3.198	2.973	3.026
	3.165	3.484	3.360	3.224	3.221
X6 \cdots M \cdots X6	159.7	163.2	163.3	162.5	162.7
	154.0	159.4	158.8	161.6	161.9
av. N–N–C–Cl	4.1	7.5	8.6	12.2	12.7
	3.6	5.9	9.2	15.9	16.2

standard functionals like the Becke-type functional B3LYP or the Perdew-type functional MPW1PW91 but also Truhlar’s MPW1B95 functional.^{32c} The latter was developed and adapted for systems with a high degree of noncovalent bonding. Increasing computer power allows it to study, at least at the DFT level, not only simple model compounds but also experimentally accessible systems as the biphenyl substituted potassium and thallium triazenides MN₃Tph₂ (**2a**, **3a**). Table 4 summarizes selected experimental and DFT-calculated bond parameters for **2a** and **3a**. In general, there is a reasonably good agreement between the calculated and experimental M–N and N–N bond lengths with relative differences of 0.8% and 1.0%, respectively. However, calculations using the functional B3LYP fail to reproduce the M \cdots C distances, which are considerably overestimated by +5.5% (**2a**) and +8.5% (**3a**). Slightly better but still unacceptable results are obtained with the functional MPW1PW91 [+4.0% (**2a**) and +8.5% (**3a**)]. The use of Truhlar’s MPW1B95 functional greatly improves the results, the Tl \cdots C distances are now overestimated by +1.5% whereas the K \cdots C distances are underestimated by –2.3%. The best results for the K \cdots C distances with a relative error of –0.9% are obtained by adding diffuse functions to the lighter atoms N, C, and H.⁴³

Further insights about the different bonding situation in **2a** and **3a** are provided by natural bond orbital (NBO) and NPA (natural population analysis) analyses.^{32g} For **2a**, the high NPA charge of +0.889 on K and the low Wiberg bond orders^{32h} of 0.037 and 0.029 for the K–N1/N3 and K–N2 bonds are in accordance with the mainly ionic character of these bonds. For **3a**, a higher degree of covalent bonding is reflected by a NPA charge of +0.698 on Tl and relatively higher Wiberg bond orders of 0.085 and 0.074 for the Tl–N1/N3 and Tl–N2 bonds, respectively. A similar trend is observed for the M \cdots C bonding that is much weaker, however, with small Wiberg bond orders in the range 0.003–0.006 (K \cdots C) and 0.009–0.018 (Tl \cdots C). The nevertheless shorter K \cdots C distances are a result of stronger Coulomb contributions as reflected by the different NPA charges on K or Tl on one side and the π -bonded Trip arene rings (average total charges: C₆H₂iPr₃ ring, –0.013 {**2a**}, +0.040 {**3a**}; C₆H₂ fragment, –0.116 {**2a**}, –0.089 {**3a**}) on the other side. A close examination of possible interactions between filled (donor) NBOs and empty (acceptor) NBOs

(43) For the B3LYP and MPW1PW91 calculations, the addition of diffuse functions leads to even larger relative errors.

by second-order perturbation theory reveals no significant charge delocalization from the lone pair on Tl (with 99.3% s-character) to suitable ligand centered acceptor orbitals.

Conclusion

In summary, we have used sterically crowded, triazenido ligands to stabilize monomeric and dimeric, unsolvated complexes of potassium and thallium. Remarkably, those homologous complexes appear to be the first examples of molecular species with the same composition that crystallize in isomorphous cells. The different nature of the M–N and M···C(arene) bonding was studied by DFT calculations that

show a higher degree of covalence for the thallium compounds and no significant influence from the lone pair on Tl.

Acknowledgment. We thank the Deutsche Forschungsgemeinschaft (SPP 1166) for financial support.

Supporting Information Available: A figure that illustrates structural differences of known molecular K and Tl compounds, computational data for **2a** and **3a**, molecular structure plots of **2a–d**, **2d** (cyclopentane)_{1.5} (PDF), and X-ray data (CIF) for **2a–d**, **3a–d**, and **2d** (cyclopentane)_{1.5}. This material is available free of charge via the Internet at <http://pubs.acs.org>.

IC800029Z